

Continuous Twisted Nanofiber Yarns Fabricated by Double Conjugate Electrospinning

Jianxin He^{1,2*}, Yuman Zhou^{1,2}, Kun Qi², Lidan Wang², Pingping Li¹, and Shizhong Cui¹

¹College of Textiles, Zhongyuan University of Technology, Zhengzhou 450007, P.R. China

²Henan Key Laboratory of Functional Textile Materials, Zhongyuan University of Technology, Zhengzhou 450007, P.R. China

(Received November 4, 2012; Revised April 20, 2013; Accepted May 17, 2013)

Abstract: In order to fabricate continuously twisted nanofiber yarns, double conjugate electrospinning had been developed using two pairs of oppositely charged electrospinning nozzles. The principle and process of this novel yarn spinning method were analyzed, and the effect of applied voltage, nozzle distance between positive and negative, solution flow rate and funnel rotating speed on the diameters, twist level and mechanical properties of resultant PAN nanofiber yarns were investigated in this paper. The results indicated that electrospun nanofibers aggregated stably and bundled continuously at the applied voltage of 18 kV, the nozzle distance of 17.5 cm between positive and negative, the overall flow rate of 3.2 ml/h and the flow ratio of 5/3 for positive and negative nozzles. The resultant nanofiber yarns had favorable orientation and uniform twist distribution, and the twist level of nanofiber yarns increased with the increase of the ratio of funnel rotating speed and winding speed. The diameters and mechanical properties of nanofiber yarns depended on their twist level. The diameters of prepared PAN nanofiber yarns ranged from 50 μm to 200 μm , and the strength and elongation of PAN nanofiber yarns at break were 55.70 MPa and 41.31%, respectively, at the twist angle of 41.8°. This method can be also used to produce multi-functional composite yarns with two or more components.

Keywords: Nanofiber, Yarn, Double conjugate, Electrospinning, Tensile property

Introduction

Electrospinning had been demonstrated to be a simple and viable method to produce fibers with diameters in the nanometer to sub-micrometer size range from polymer solution. Electrospun nanofibers with nanometric diameter, large specific surface area and small pore size had been found vast application potential in protective clothing, biomaterials, tissue scaffolds, nanocomposites, sensor and filtration [1,2]. However, most of electrospun fibers were produced in the form of randomly oriented nonwoven fiber mats. The relatively low mechanical strength and the difficulty in tailoring the fibrous structure had restricted their applications. Hence, there is a considerable interest in the development of continuous yarns made out of nanofibers, which provide an attractive way to incorporate polymeric nanofibers into traditional textiles with broader market. To be brief, nanofiber yarn is defined as a twisted nanofiber bundle or tows having morphology like filament yarn or spun yarn, which is mechanically suitable for weaving, knitting and other methods of producing a fabric [3].

In recent years, many attempts have been made to produce yarns from nanofibers [4,5]. Electro-wet spinning developed by Khil [6] and Smit *et al.* [7] deposited nanofibers into coagulating bath to eliminate the charges of the charged nanofibers, and the fiber bundles formed on the liquid surface were drawn out under the action of liquid surface tension. The electro-wetting technique was greatly enhanced by Teo *et al.* [8] Nanofiber web was firstly electrospun from

a polymer solution onto the surface of a solution within a cylindrical container, and then the fiber web was drawn and twisted into nanofiber yarn using a vortex fluid flow located in the bottom of the cylindrical container. Continuous nanofiber yarns could be obtained through electro-spun wet spinning, but nanofibers exhibited bad orientation and arrangement in the yarns [9]. In addition, this method was only fit for polymer nanofibers that could deposit on conductive coagulating bath.

Some researchers produced twisted nanofiber yarns using dynamic mechanical collector [10,11]. Afifi *et al.* [12,13] used a slowly rotating grounded “funnel” to collect electrospun fiber yarns. The charged jet was ejected toward the grounded funnel target from a diagonal direction to form a web on the mouth plane. The web was twisted as it was formed, and pulled upward to the winder. Bazbouz and Stylios [14] improved the gap collector by using two perpendicularly disks placed 4 cm apart. One disk was rotated to twist the nanofibers, and the other was served for continuous yarn winding. Other researchers produced twisted nanofibers by controlling the whipping jet and using a modified electric field from an auxiliary electrode or the manipulation of the electric field [15]. However, issues remained with these methods in controlling the twist level, yarn dimension and spinning stability.

More recently, Dabirian and Hosseini [16], Ali [17], Li *et al.* [18,19] developed a process referred to as conjugated electrospinning. The nanofiber bundles were aggregated and twisted by rotating unearthed metal disc or funnel placed in the middle of two opposite polarity nozzles. Li *et al.* [20] fabricated electrospun nanofiber yarn by using a funnel-

*Corresponding author: hejianxin771117@163.com

shape collector with airflow, and found that LiCl additives were beneficial to PAN fiber convergence and yarn structure.

In this paper, a modified method of conjugated electrospinning referred to as double conjugate electrospinning were applied to produce continuous PAN nanofiber yarns with a well-controlled twist level, and the principle and process of this spinning method were investigated thoroughly.

Experimental

Materials

Polyacrylonitrile (PAN, M_w 60,000) and N-N dimethyl formamide (DMF) were supplied by Shanghai Chemical Reagent Co. Ltd., China.

Preparation of Spinning Solution

PAN solution of 15 wt% concentration was prepared through dissolving PAN powder in DMF solution at 80 °C for 3 h.

Spinning Continuous Nanofiber Yarn

Double conjugate electrospinning set-up used to spinning continuous nanofiber yarns is shown in Figure 1, including two fluid supply apparatus, a stainless steel funnel collector, two liquid transport tubes, four needle nozzles, a yarn winder and a high voltage DC power supply. A couple of liquid transport tubes equipped with two nozzles, which connected separately with the positive and negative electrodes of the DC power supply, arranged symmetrically on both sides under funnel collector. The funnel collector was unearthed.

PAN solution was transported to needle nozzles with uniform rates through liquid transport tubes by fluid supply apparatus. Nanofibers electrospun from the oppositely charged nozzles were deposited onto the rotary funnel to form a nanofiber web that covers the funnel end. By the drawing of an insulating rod, the nanofiber web was pulled

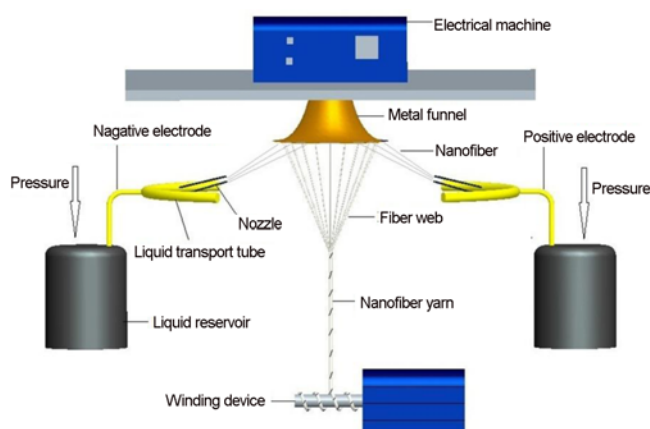


Figure 1. The schematic of double conjugate electrospinning device for preparing nanofiber yarns.

into fiber bundle. Then the fiber bundle was twisted by rotary funnel and wound continually to yarn winder.

A voltage of 14–22 kV was applied to the nozzles with the distance from the tip of the nozzle to the side of the funnel mouth at 4 cm. The distance between positive and negative nozzles ranged from 14 to 20 cm. The overall flow rate of spinning solution was varied from 2.0 to 4.4 ml/h and the flow ratio of positive and negative nozzle varied from 3/5 to 3/2. Revolution per minutes of funnel collector was adjusted in the range of 0–180 r/min, and take-up speed of yarn winder was 40 cm/min.

Characterizations

The nanofiber yarns collected were coated with gold film in order to observe fiber and yarn morphologies. The instrument was a JEOL JSM-5600LV electron microscopic with an accelerating voltage of 10 kV. The diameters of fiber and yarn and the twist angle were calculated based on the SEM images. At least 100 counts were taken for each measurement.

Mechanical Property Measurement

The tensile properties were measured with an INSTRON 365 tester at room temperature under room humidity. The gauge length was set to 10 cm and the rate of the crosshead was 100 mm/min. The reported data of breaking strength and elongation represent the average results of 30 tests.

Results and Discussion

Spinning Mechanism and Process

The electric field distribution between the nozzles and the funnel collector for non-conjugate and conjugate electrospinning were simulated by Maxwell12.0 software and compared as shown in Figure 2. Figure 2(a) shows the electric field simulation of non-conjugate electrospinning, in which the needle nozzles in both groups were positively charged while the stainless steel funnel was negatively charged. The electric field forms between the funnel collector and four needle nozzles, and the electric field lines direct from nozzle tip to inner and outer surfaces of funnel. During electrospinning, nanofibers ejected from four needle nozzles move and adhere to the inner and outer surfaces of funnel. Owing to having same charge for these fibers, the strong repulsive forces among the fibers make them unable to form a hollow fiber web, thereby unable to spin continuous yarns.

Figure 2(b) shows the electric field simulation of conjugate electrospinning, in which two pairs of needle nozzles were positively and negatively charged, respectively, and the funnel collector was not earthed. After applying voltage, the electric field comes into being between positive and negative nozzles; however, the steel funnel located in the middle of two groups of nozzles will change the original distribution of electric field. Electrostatic induction makes both edges of

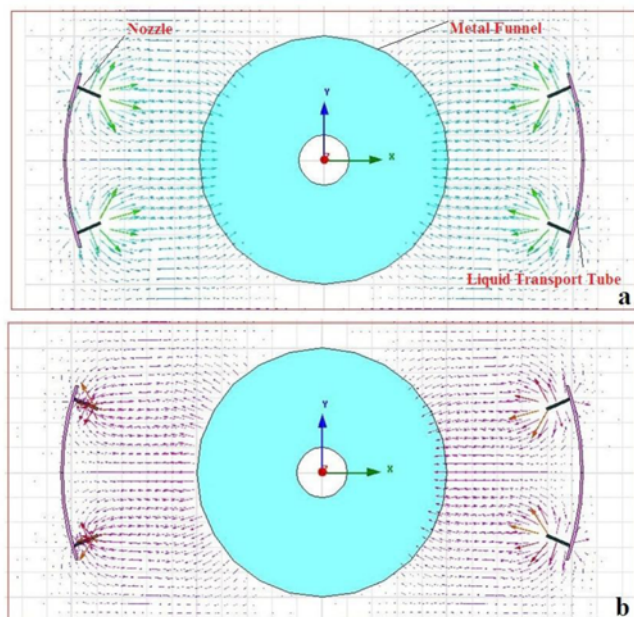


Figure 2. Electric field simulation of double (a) non-conjugate electrospinning and (b) conjugate electrospinning.

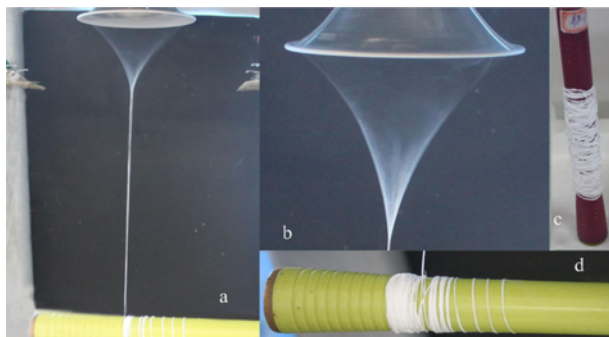


Figure 3. Experimental images of preparing nanofiber yarns by double conjugate electrospinning; (a) the schematic of preparing continuous nanofiber yarns, (b) inverted cone-shaped hollow fiber web, (c) electrospun nanofiber yarn product, and (d) winded nanofiber yarn.

the funnel have the charges that are opposite to the nearby charged nozzles, thereby there have been induction fields between both edges of the funnel and their nearby charged nozzles. The charged jets ejected from two pairs of oppositely charged nozzles would be attracted towards the side of the inductive funnel with opposite charges, and then the jets got neutralized and formed a hollow nanofiber web composed of plenty of nanofibers from positive and negative nozzles with its edges connecting to the funnel end (Figure 3(b)). After drawn by an insulating rod placed beforehand near the central area of the funnel, the hollow nanofiber web formed a ‘fibrous cone’ with its apex attaching to the rod. Further drawing the cone apex induced the formation of orientated

fiber bundle, which was twisted by rotating funnel and winded onto the winder as continuous yarns (Figure 3).

In this case, once the fibrous cone was created, the subsequent electrospun nanofibers could actually deposit between the fibrous ‘cone’ and the funnel collector. The use of oppositely charged nanofibers facilitated the formation of stable nanofiber ‘cone’ because of electrostatic interaction.

In the experiment, the key to produce continuous nanofiber yarn for the novel double conjugate electrospinning with two pair’s nozzles is the formation of stable fibrous cone during the yarn spinning process. The study has found that the applied voltage, the nozzle distance between positive and negative, the solution flow rate and the funnel rotating speed affected not only the stability of the fibrous ‘cone’ but also the fiber and yarn diameters, as well as the twist level and the quality of the yarn.

Effect of Applied Voltage on Nanofiber and Yarn Diameters

Similar to conventional electrospinning process, spinning nanofiber yarns by double conjugate electrospinning also needed the applied voltage to be above a critical value. When the applied voltage was lower than 14 kV, no yarns were formed and only a small amount of nanofibers deposited on the funnel collector, apparently due to insufficient nanofibers produced. When increasing the applied voltage to 18 kV, a continuous nanofiber web would be formed stably and the nanofiber yarn could be withdraw from the top of the web cone continuously. By further increasing the applied voltage, spinning nanofiber yarn by electrospinning was maintained in a steady state. However, when the applied voltage was above 22 kV, nanofibers were easy to flow into the air and difficult to deposit onto the funnel collector, thus nanofiber yarn could not be spinning continuously again. It was found that when the applied voltage was 18 kV, the inverted cone-shaped hollow fiber web and fiber bundle were formed best. Nanofiber yarn spinning could keep stable well and broken ends hardly occurred in this condition.

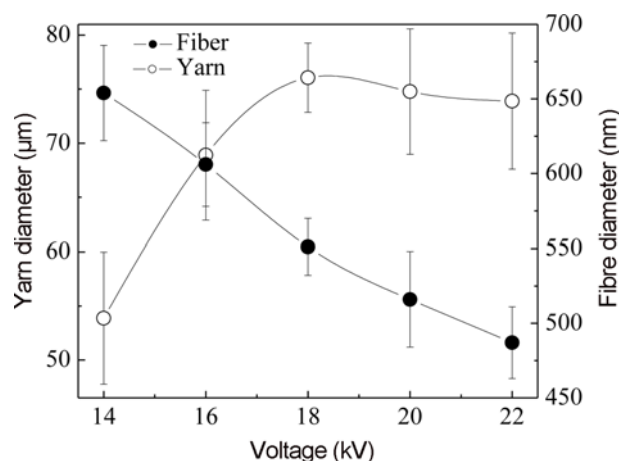


Figure 4. Effect of applied voltage on nanofiber and yarn diameters.

The dependences of the nanofiber and yarn diameters on applied voltage are shown in Figure 4. Nanofiber diameters decreased with the increase of applied voltage, whereas the yarn diameters increased. When the voltage increased up to 18 kV, nanofiber yarn diameters exhibited a maximal value of 76 μm . The increased yarn diameters can be explained by the increase of fiber scales due to the increase of applied voltage. However, by further increasing the applied voltage, the yarn diameters had been reduced when the voltage exceeded 18 kV. This can be explained by the reduction in nanofiber deposition on the funnel collector under such a high voltage, which could derive from the unbalanced charges between the nanofibers generated from the two pairs of nozzles and associated charge accumulation on the funnel collector.

Effect of Nozzle Distance Between Positive and Negative on Nanofiber and Yarn Diameters

The nozzle distances between positive and negative affected the intensity of electric field. When the applied voltage remained constant, reducing the nozzle distance between positive and negative led to the increase of electric field strength. Under a stronger electric field, fibers travelled faster. The adhesion among incomplete volatile fibers limited the slipping of fibers, resulting in the decrease of the stability of hollow fiber web. Therefore, the fibers were easy to conglutinate on the funnel collector and hard to be drawn into a uniform yarn. In contrast, increasing the nozzle distance between positive and negative also reduced the spinnability of nanofiber yarn due to reduced fiber deposition on the funnel induced by the decreased field strength. In addition, there existed jet exclusion between the nozzles with the same charge, which affected the spinning stability of nanofiber yarn.

In the experiments, when applied voltage remained constant, the fibers could not be deposited on the funnel, but attracted to the negative electrode at the nozzle distance between positive and negative less than 14 cm. When the nozzle distance between positive and negative was greater than 20 cm, the fibers from the needle nozzles reduced, thus the yarns could not be generated stably again. Nanofiber yarns could be electrospun stably when the nozzle distance between positive and negative was 17.5 cm, and the distance between homopolar nozzles was 5.5 cm.

Figure 5 shows the dependence of nozzle distance between positive and negative on nanofiber and yarn diameters. Nanofiber diameters increased with the increase of nozzle distance between positive and negative. Increased nozzle distance between positive and negative weakened the intensity of electric field and the drafting force. Furthermore, smaller voltage of 18 kV was used in the experiment when analyzing nozzle distance between positive and negative. Thus the intensity of electric field played an important role on nanofiber diameters and the increase of nozzle distance

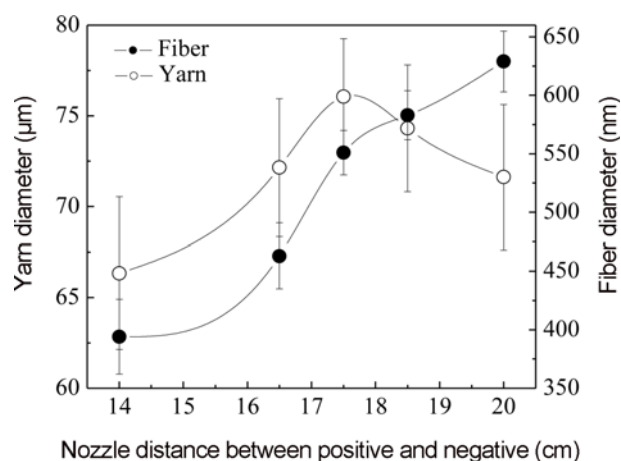


Figure 5. Effect of nozzle distance between positive and negative on nanofiber and yarn diameters.

between positive and negative led to the increase of nanofiber diameters. With the increase of the nozzle distance between positive and negative, the yarn diameters increased initially and exhibited a maximal value of 76 μm at the nozzle distance of 17.5 cm. In the case of less nozzle distance between positive and negative, some incomplete volatile fibers, induced by faster travel of fiber under a stronger electric field, were hard to be drawn into a uniform yarn, but attracted to the negative electrode; thereby the nanofiber yarn had a thinner diameter. As nozzle distance between positive and negative increased, the full draft of nanofibers in electric field increased the amount of fiber adsorbed on the fiber web, and the yarn diameters gradually increased. When nozzle distance between positive and negative was greater than 17.5 cm, by further increasing the distance, the yarn diameters reduced because of the decreased fiber deposition rate under a weak electric field.

Effect of Solution Flow Rate on Nanofiber and Yarn Diameters

The ratio of the flow rates between positively and negatively charged nozzles (F_p/F_N) was found to be an important parameter influencing the yarn spinning process. As already reported by the literature, nanofiber production from the positively charged nozzles is about 1.6 times higher than that from the negatively charged nozzles because the electric field in the positively charged electrospinning process is stronger [21]. When the overall flow rate remains unchanged, the nanofibers would have a smaller diameter if the flow ratio of positive nozzles was higher than that of the negative, whereas the fiber diameters would increase and bead fibers would be existed if the flow ratio of negative nozzles was higher than that of the positive. Hence, nanofiber yarn spinning could keep stable well with higher flow rate from the positively charged nozzles. Nanofiber production was supplied sufficiently and the fiber web formed best when $F_p/$

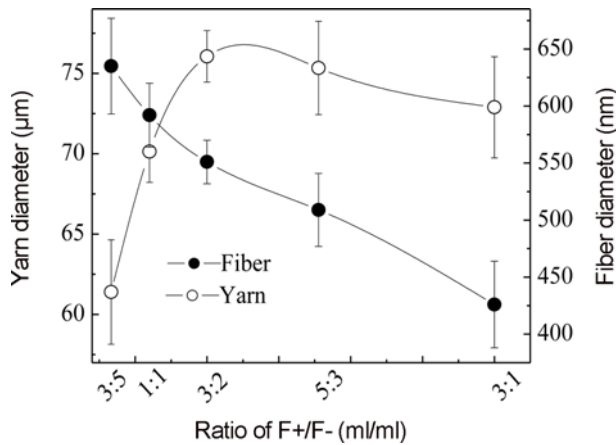


Figure 6. Effect of the ratio of the flow rates between positively and negatively charged nozzles on nanofiber and yarn diameters.

F_N was 5/3.

The dependence of F_p/F_N on nanofiber and yarn diameters is shown in Figure 6. When overall flow rate kept a constant of 3.2 ml/h, nanofiber diameters decreased with the increase of F_p/F_N , whereas yarn diameters increased. Nanofiber yarn diameters reached to a maximal value of 76 μm at F_p/F_N of 5/3. However, by further increasing F_p/F_N , yarn diameters decreased. When F_p/F_N was less than 5/3, less fiber scales, derived from excessive solution dropped from negative charged nozzle and insufficient solution supplied from positive, reduced the diameters of nanofiber yarns. On the other hand, when F_p/F_N was more than 5/3, it existed a

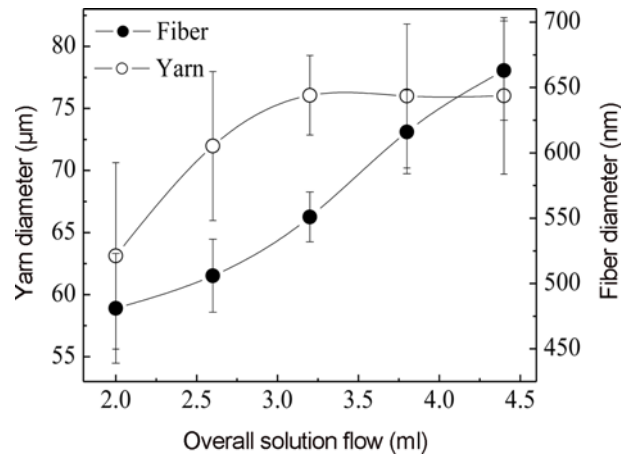


Figure 7. Effect of overall flow rate on nanofiber and yarn diameters.

opposite phenomenon that excessive solution dropped from positive charged nozzle and insufficient solution supplied from negative.

When F_p/F_N remained a stable value of 5/3, if overall flow rate was lower than 2 ml/h, the fiber web would be unstable and uneasy to form fiber bundles due to insufficient supplied solution. There was no excessive solution dropped from nozzles and fiber web was uniform, stabilized and continuous at the overall flow rate of 3.2 ml/h. However, when overall flow rate exceeded 3.2 ml/h, excessive solution dropped from the tip of nozzle, nozzles and fiber web were conglomerated by many incomplete volatile fibers.

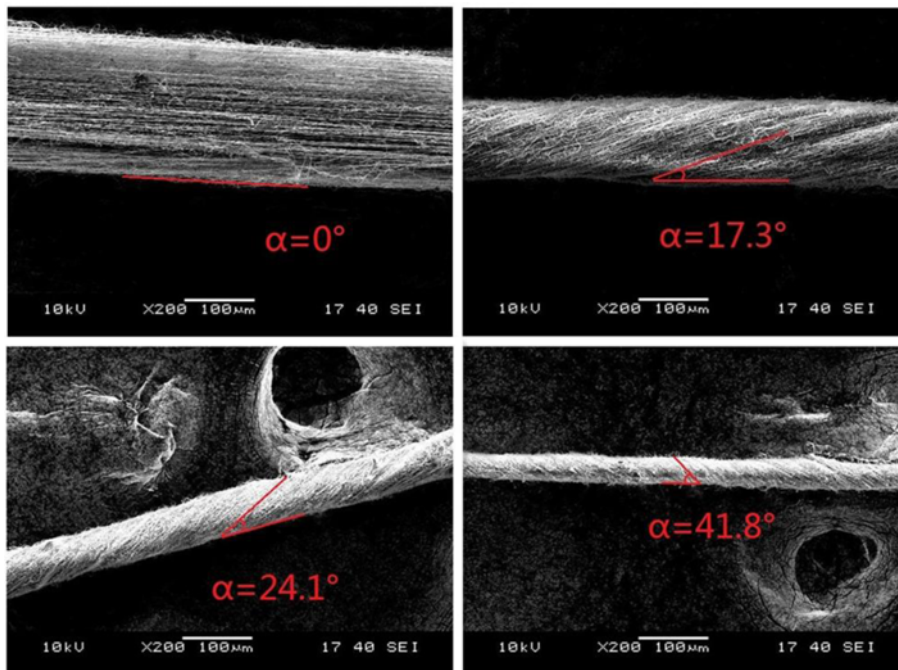


Figure 8. SEM photographs of nanofiber yarns on different S_p/S_w .

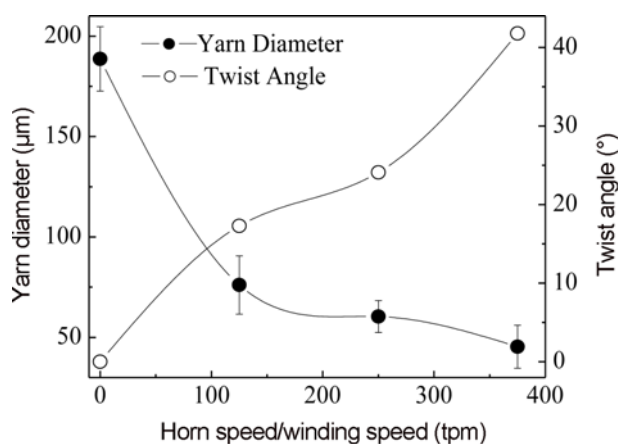


Figure 9. Effect of the ratio of funnel speed and winding speed on twist angles and diameters of nanofiber yarns.

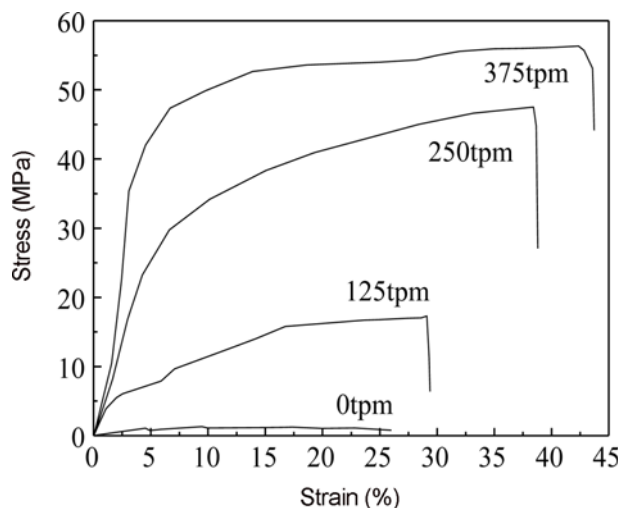


Figure 10. Tensile curve of nanofiber yarns on different twisting levels.

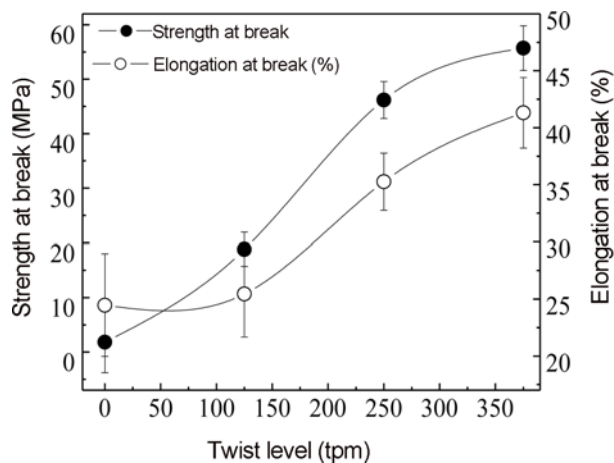


Figure 11. Effect of twist level on strength and elongation of nanofiber yarns at break.

Figure 7 shows the dependence of overall flow rate on nanofiber and yarn diameters. When F_p/F_N was 5/3, if overall flow rate exceeded 3.2 m³/h, nanofiber diameters would increase with the increase of overall flow rate, but the yarn diameters would increase first and then sustained stable. In addition, unordered nanofibers were found on yarn surfaces.

Effect of Twisting on Diameter and Mechanical Property of Nanofiber Yarn

Aggregation, bundle and twisting of nanofibers were accomplished through unearthed metal funnel; thereby yarn diameters and twist level are dependent on the ratio of funnel speed and winding speed (S_F/S_W). The morphology of nanofiber yarns on different S_F/S_W was shown in Figure 8. Continuous nanofiber bundles could be obtained when the funnel kept motionless and fibers had a good parallelism in bundles. Twisted nanofiber yarns could be produced when the funnel was rotating, and uniform twist distribution could be observed on yarn surfaces. Yarn diameters decreased from 188.6 to 45.3 μm, whereas twist angle increased from 0° to 41.8° with the increase of S_F/S_W from 0 to 375 tpm (Figure 9).

Similar to conventional textile yarns, twisting is a key factor to yarn having mechanical property. Untwisted yarn hardly displayed mechanical properties. However, mechanical properties of twisted yarns enhanced obviously with the increase of twist level. Tensile curves of nanofiber yarns are composed of linear hookean zone and yield zone (Figure 10). The strength of yarns maintains stable, but the elongation increases after yielding. Initial modulus increases and yield points move backward with the increase of nanofiber yarns in twist level. Strength and elongation at break increased from 1.81 to 55.70 MPa and from 24.47% to 41.31%, respectively (Figure 11). Untwisted yarn showed weaker a cohesion force among nanofibers. The slipping of nanofibers caused the fracture of yarn easily, and the elongation of yarn was dependent on the distance of fiber slipping. Twist level of yarn increased with the increase of S_F/S_W , and the cohesion force and frictional resistance among fibers in twisted yarns increased signally with the increase of twist level. Hence, the strength and elongation at break increased with the increase of twist level.

Conclusion

Double conjugate electrospinning device was designed to produce continuous twisted nanofiber yarns. Nanofiber yarn diameters increased first and then decreased with the increase of applied voltage, nozzle distance between positive and negative and F_p/F_N . However, with the increase of overall flow rate, yarn diameters increased first and then remained stably. Nanofiber yarns could be produced continuously and stably at the applied voltage of 18 kV, the nozzle distance of 17.5 cm between positive and negative, the overall flow rate

of 3.2 ml/h and the F_p/F_N of 5/3. The diameters of yarns decreased, but twist level and mechanical property increased by increasing S_F/S_W . The strength and elongation at break were 55.70 MPa and 41.31% respectively at twist angle of 41.8° . Multiple conjugate electrospinning will be researched in later experiment, and new method will be proposed for production and application of nanofiber yarns.

Acknowledgement

This work was supported by a grant from National Natural Science Foundation of China (No. 51203196), and the financial support of the United Foundation from National Natural Science Foundation of China and The People's Government of Henan Province for Cultivating Talents (No. U1204510) is gratefully acknowledged.

References

1. Z. M. Huang, Y. Z. Zhang, and M. Kotakli, *Compos. Sci. Technol.*, **63**, 2223 (2003).
2. C. B. Huang, S. L. Chen, C. L. Lai, D. H. Reneker, H. Y. Qiu, Y. Ye, and H. Q. Hou, *Nanotechnology*, **17**, 1558 (2006).
3. F. L. Zhou and R. H. Gong, *Polym. Int.*, **57**, 837 (2008).
4. C. K. Liu, R. J. Sun, K. Lai, C. Q. Sun, and Y. W. Wang, *Mater. Lett.*, **62**, 4467 (2008).
5. F. Ko, Y. Gogotsi, A. Ali, N. Naguib, H. Ye, G. L. Yang, C. Li, and P. Willis, *Adv. Mater.*, **15**, 1161 (2003).
6. M. S. Khil, S. R. Bhattarai, H. Y. Kim, S. Z. Kim, and K. H. Lee, *J. Biomed. Mater. Res. B.*, **72**, 117 (2005).
7. E. Smit, U. Buttner, and R. D. Sanderson, *Polymer*, **46**, 2419 (2005).
8. W. E. Teo, R. Gopal, R. Ramaseshan, K. Fujihara, and S. Ramakrishna, *Polymer*, **48**, 3400 (2007).
9. Z. J. Pan, H. B. Liu, and Q. H. Wan, *J. Fiber Bioeng. Inform.*, **1**, 47 (2008).
10. K. Zhang, X. F. Wang, Y. Yang, L. L. Wang, M. F. Zhu, S. Benjamin, and B. Chu, *J. Polym. Sci. Pol. Phys.*, **48**, 1118 (2010).
11. Y. Hao, L. Q. Liu, and Z. Zhang, *Mater. Lett.*, **65**, 2419 (2011).
12. A. M. A, S. Nakano, H. Yamane, and Y. Kimura, *Macromol. Mater. Eng.*, **295**, 660 (2010).
13. S. F. Fennessey and R. J. Farris, *Polymer*, **45**, 4217 (2004).
14. M. B. Bazbouz, Ph. D. Dissertation, HWU, Edinburgh, 2009.
15. F. Q. Sun, C. Yao, T. Y. Song, and X. S. Li, *J. Text. I.*, **102**, 633 (2011).
16. F. Dabirian, S. A. H. Ravandi, R. H. Sanatgar, and J. P. Hinestroza, *Fiber. Polym.*, **12**, 610 (2011).
17. U. Ali, Y. Q. Zhou, and T. Lin, *J. Text. I.*, **103**, 80 (2012).
18. H. Pan, L. M. Li, L. Hu, and X. J. Cui, *Polymer*, **47**, 4901 (2006).
19. M. S. M. Jad, S. A. H. Ravandi, H. Tavanai, and R. H. Sanatgar, *Fiber. Polym.*, **12**, 801 (2011).
20. N. Li, Q. Hui, H. Xue, and J. Xiong, *Mater. Lett.*, **79**, 245 (2012).
21. A. Kilic, F. Oruc, and A. Demir, *Text. Res. J.*, **78**, 532 (2008).